Anal. Bioanal. Chem. 401 (2011) 1963–1974

Surface-assisted laser desorption/ionization-mass spectrometry using TiO_2-coated steel targets for the analysis of small molecules

H. Sonderegger[1], C. Rameshan[2,3], H. Lorenz[2], F. Klauser[2], M. Klerks[1], M. Rainer[1], R. Bakry[1], C. W. Huck[1], G. K. Bonn[1]*

[1] Institute of Analytical Chemistry and Radiochemistry, Leopold-Franzens University, Innsbruck, Austria
[2] Institute of Physical Chemistry, Leopold-Franzens University, Innsbruck, Austria
[3] Department of Inorganic Chemistry, Fritz-Haber-Institute of the Max-Planck-Society, Berlin, Germany

* Corresponding author: e-mail guenther.bonn@uibk.ac.at,

Received: 6 May 2011; Revised: 8 July 2011; Accepted: 13 July 2011; Published online: 31 July 2011

Abstract

Matrix-assisted laser desorption/ionization-mass spectrometry (MALDI-MS) measurements in the low-molecular mass region, ranging from 0 to 1000 Daltons are very often difficult to perform because of signal interferences originating from matrix ions. In order to overcome this problem, a stainless steel target was coated with a homogeneous titanium dioxide layer. The layer obtained was further investigated for its ability to desorb small molecules, e.g. amino acids, sugars, polyethyleneglycol (PEG 200) or extracts from *Cynara scolymus* leaves. The stability of the layer was determined by repeated measurements on the same target location, which was monitored by X-ray photoelectron spectroscopy (XPS) and scanning electron microscopy (SEM) before and after surface assisted laser desorption/ionization (SALDI) analysis. In addition, the titanium dioxide layerwas compared with an already published method with titanium dioxide nanopowder as inorganic matrix. As a result of this work, the titanium dioxide layer produced minimal background interference, enabling simple interpretation of the detected mass spectra. Furthermore, the TiO_2 coating provides a target that can be reused many times for SALDI-MS measurements.

Keywords: MALDI; LDI–MS; SALDI; TiO_2 coating; Metabolites

1. Introduction

For the analysis of biological and synthetic macromolecules matrix-assisted laser desorption/ionization mass spectrometry has become widely used during the last two decades. MALDI, a soft ionisation method, was first by Karas and Hillenkamp in 1988 [1-3]. A successful MALDI measurement is strongly affected by selection of the appropriated matrix, which is responsible for the ionization of the sample molecules. Unfortunately, selection of the correct matrix is still based on empirical data, therefore, scientists have put much effort into developing new matrices [4].

In general, the applied matrix consists of a low-molecular-weight organic compound able to absorb the energy of a pulsed laser light. Cinnamic acid derivatives and aromatic carbonyl derivatives are the two major classes of organic matrices for MALDI measurements [5,6]. In conventional MALDI analysis many variables which may affect the integrity of good, homogeneous sample preparation include the concentration of matrix and analyte, choice of matrix, temperature and solubility. Although organic acid matrices are usually preferred because of their high sensitivity and ionization efficiency, a major drawback is the generation of background signals in the low mass range (<700 *m/z*) making it difficult to analyze low-molecular-weight compounds. Because of this limitation, a significant amount of work has been undertaken in recent years to develop laser desorption/ionization techniques that can be performed without conventional matrices.

A first attempt was to use an inorganic matrix, for example metal particles. The major advantage herein is the absence of matrix interferences in the mass range below 1000 *m/z*. Tanaka et al. first introduced a novel ionization technique in which cobalt powder was mixed with glycerol and applied as matrix [7]. Cobalt powder 30 nm diameter was mixed with the analyte and suspended in glycerol, and

the resulting mixture was irradiated with a pulsed nitrogen laser. Tanaka described the properties of cobalt nano-powder as follows: high photo-absorption, large surface area per particle and low heat capacity. Because of the low heat capacity the cobalt particles enable rapid heating [8], which is needed for desorption and ionization of analyte molecules without thermal decomposition.

Schürenberg et al. [9] were inspired by Tanaka´s work and investigated several nanoparticles like graphite, iron oxide or titanium nitride as matrices for the analysis of proteins and peptides. Dale et al. [10,11] and Sunner et al. [12] compared the performance of micro- and nanoparticles as inorganic matrices. Sunner et al. introduced the term SALDI (Surface-Assisted Laser Desorption/Ionization) as a differentiated technique from MALDI in which organic matrices are used. One major advantage of SALDI-based systems is that there is no need for organic acid matrices which eliminates all inhomogeneities regarding matrix/analyte co-crystallization caused by sample preparation. The exact mechanism of laser desorption/ionization in SALDI-based systems is yet not completely understood, but the physical characteristics of nano-structured surfaces including their thermal, electric and chemical properties are supposed to have a large effect on energy absorption and transfer [13]. The thermal properties, especially, contribute to this process. It is observed that local temperatures of the nano-structured surface are increased on laser irradiation. This extra heat is then transferred to the analytes to bring them into the gaseous phase [14].

Crecelius et al. [15] reported the successful application of particle suspensions as matrices for the analysis of tetracycline antibiotics by thin-layer chromatography matrix-assisted laser desorption/ionization time-of-flight mass spectrometry (TLC–MALDI–TOF–MS). In Crecelius work particles of different materials and sizes have been investigated (Co-UFP, TiN, TiO_2, graphite and silicon) by applying two particle suspensions to eluted TLC plates. Kawasaki et al. used gold nanoparticles for the successful ionization of proteins and low molecular weight species [16].

Michalak et al. [17] discovered that C_{60} fullerenes are suitable matrix candidates for protein analysis. This was confirmed by Huang et al. [18] who used them for screening urine for diuretics. Szabo et al. [19] derivatized silica with C_{60} fullerene and investigated the product for LDI analysis of carbohydrates, amino acids, peptides, phospholipids and drugs.

Armstrong et al. and Li et al. [20,21] introduced the term ILM for ionic liquid matrices for LDI-MS analysis of phospholipids. They claimed that ILMs have advantages over the crystalline 2,5–DHB matrix. Use of these ionic liquid matrices leads to higher signal intensity, comparable or better sensitivity, and improved sample homogeneity, providing better signal reproducibility.

Najam-ul-Haq et al. [22] introduced a nanostructured diamond-like carbon (DLC)-coated digital versatile disk (DVD) target as a matrix-free sample support for laser desorption/ionization mass spectrometry (LDI-MS) [22].

A porous silicon surface has also been used for LDI-MS, which is referred to as desorption/ionization on silicon (DIOS) [23-27]. For DIOS-MS, porosity or roughness is presumed to be necessary for desorption/ionization [28,13,29,30]. In DIOS-MS, the dissolved analytes are deposited directly on the silicon surface without an additional matrix. DIOS is often termed “matrix-free” LDI to emphasize its advantages, for example the absence of low mass interferences caused by matrix ions [31-35].

More recently, direct laser desorption/ionization on carbon nanotubes or silicon nanowires has been reported [36,37].

Kinumi et al. [38] investigated the applicability of several metal and metal oxide micro particles (Al, Mn, Mo, Si, SnO_2, TiO_2, W, WO_3, Zn and ZnO_2) as inorganic matrix for the analysis of small molecules.

Among the materials tested, TiO_2 powder turned out to be the most promising medium for detection of low-molecular-weight analytes, because of its strong absorption in the UV range.

Taking advantage of the strong spectral absorption of TiO_2 in the UV range, mesoporous nanocrystalline TiO_2 sol–gel has also been used to detect large proteins, for example trypsinogen [39]. Another approach using TiO_2 as photoabsorbing material has been developed in recent years. Bi et al. developed a single-use aluminum foil-based laser desorption/ionization (LDI) target plate for mass spectrometry (MS) [40]. Arrays of TiO_2 nanoparticle spots are coated on the foil either by screen-printing or rotogravure-printing followed by sintering to form a mesoporous layer spot to act as an anchor for sample deposition.

Mesoporous tungsten titanium oxides (MTTO) materials have been used as matrix in MALDI-MS for the detection of the cyclic decapeptide Gramicidin S [41]. The MTTO materials aid trapping of the analyte molecules while acting as energy receptacle for laser irradiation, which shows their potential application in the field of mass spectrometry.

In this study, a 50 nm layer of titanium dioxide was coated on a stainless steel target by electron beam evaporation. After the coating process, the layer was inspected by XPS (X-ray Photoelectron Spectroscopy) to calculate the stoichiometric composition of the TiO_2 film.

The main focus was put on the ability of the layer to ionize small molecules, for example amino acids, sugars and polyethylenglycol. Furthermore, an extract derived from pressed *Cynara Scolymus* leaves was analyzed. The stability of the layer was tested by performing extensive washing steps with different solvents and by performing multiple measurements on the same spot.

2. Experimental

2.1. Chemicals and reagents

L-Alanine, L-Arginine monohydrochloride, L-Asparagine anhydrous, L-Aspartic acid, L-Cysteine, L-

Glutamine, L-Glutamic acid, Glycine, L-Histidine monohydrochloride monohydrate, L-Isoleucine, L-Leucine, L-Lysine monohydrochloride, L-Methionine, L-Phenylalanine, L-Proline, L-Serine, L-Valine, L-Tyrosine, L-Threonine and L-Tryptophane (all in ≥ 99.0% (NT) purity) and deionized water (for HPLC) were all purchased from Fluka (Buchs, Suisse). L(-)Sorbose (≥ 98.0% (sum of enantiomers, HPLC)), D(-)Arabinose (≥ 98.0%), Maltotriose (*O*-α-D-Glucopyranosyl-[1→4]-*O*-α-D-glucopyranosyl-[1→4]-D-glucopyranose, approx. 95%) Maltotetraose (*O*-α-D-Glucopyranosyl-[1→4]-*O*-α-D-glucopyranosyl-[1→4]-D-glucopyranose, 96%, for HPLC), Melibiose (6-O-α-D-galactopyranosyl-D-glucose, ≥ 98.0%, for HPLC), were purchased from Sigma Aldrich (St. Louis, MO, USA).

MALDI steel targets were purchased from Applied Biosystems (Vienna, Austria).

The titanium metal rod was obtained from Oerlikon (Balzers, Liechtenstein).

2.2. Sample preparation

Amino acids were dissolved in deionized water (1 µg/µl), and combined according to their side chain classification. All carbohydrates were prepared in aqueous solutions with a concentration of 1 µg/µl.

One millilitre freshly pressed juice from *Cynara scolymus* leaves was pipetted in a 1.5 ml tube and centrifuged. Subsequently, 500 µl of the supernatant was transferred into a separate vial and 1 µl of concentrated hydrochloric acid and 500 µl of ethyl acetate were added for liquid-liquid extraction. In the next step the ethyl acetate layer was separated and the ethyl acetate vaccum evaporated. Afterwards the precipitated compounds were redissolved in 100 µl MeOH/H_2O (1/1) and 1 µl of the prepared sample was spotted on the TiO_2 coated target.

For analysis of PEG 200 with inorganic TiO_2, methanol was used to suspend the TiO_2 particles. The ratio of particles to solvent was adjusted to 1:1 (*w/v*). The mixture was dried on a conventional MALDI steel target, glycerol and PEG 200 were then added as dispersants [38]. For the other analysis, 1 µl of sample solution was directly spotted on the TiO_2 coated target.

2.3. Mass Spectrometry

Measurements were performed by an Ultraflex I (Bruker Daltonics, Bremen, Germany) MALDI-TOF/TOF MS in reflector mode. All mass spectra were recorded by summing 500 laser shots. The laser power was adjusted between 30 and 50% of its maximal intensity (130 µJ), using a 337 nm nitrogen laser having a frequency of 50 Hz. The Flex Analysis version 2.4 provided by the manufacturer was used for data processing.

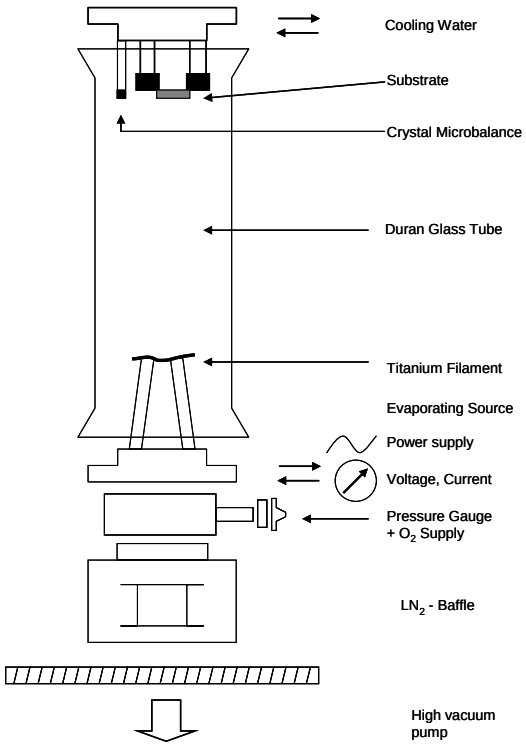

Fig. 1: Schematic drawing of the high vacuum coating chamber

2.4. Preparation and structural characterization of the TiO_2 film

All TiO_2-coated targets were prepared in a high-vacuum chamber operating at a base pressure of 10^{-4} Pa (Figure 1). Substrate temperature was set at room temperature (298 Kelvin). TiO_2 film thickness, usually 50 nm, was measured and regulated in situ by a quartz crystal microbalance. The quartz crystal was arranged symmetrically at the same height of the steel target, in order to coat the target and the crystal evenly. During the vapour deposition the changing eigenfrequency of the quartz crystal was recorded and the layer thickness calculated. Because of the well defined surface coated on the quartz crystal, one can compute the layer thickness due to the frequency modulation if the density of the evaporated metal is known (Eq. 1).

$$\frac{\Delta f}{f} = -\frac{\Delta d}{d} = -\frac{\Delta m}{(D * F * d)} \qquad (1)$$

where f is the quartz eigenfrequency, d the quartz thickness, D the quartz density, F the quartz area, and Δm the mass of the coated layer on the quartz plate.

To make sure that a stoichiometric titanium dioxide layer is formed, all films are produced in 10^{-2} Pa O_2 backpressure. After the coating process, the TiO_2 layer was inspected by XPS and SEM.

2.5. XPS

X-ray photoelectron spectroscopy was carried out at room temperature in ultra-high vacuum (base pressure $2x10^{-10}$ mbar) utilizing a Thermo MultiLab 2000 spectrometer (Thermo Scientific, Bremen, Germany) equipped with an alpha 110 hemispherical analyzer from Thermo Electron, operated in the constant analyzer energy mode at a pass energy of 100 eV. Al Spectra were collected using Al Kα radiation (1486.6 eV) monochromatized by a twin crystal monochromator yielding a focused X-ray spot with a diameter of 500 µm. The chemical composition of the layer was obtained from the areas of the detected XPS peaks in survey scans, by performing a linear background subtraction and taking into account Scofield sensitivity factors for each constituent.

2.6. SEM

The TiO_2 SALDI target was coated with gold–palladium, to a nominal depth of 10–12 nm, in a Baltech MED020 coating system and viewed in a Zeiss DSM982 Gemini field emission electron microscope operating at 5 kV

3. Results and discussion

3.1 Composition and stability analysis of the TiO_2 coated layer

To investigate the stability of the TiO_2 coating by SEM and XPS analysis, the target was exposed to laser irradiation at high energies (90 to 130 µJ).

3.1.1. Chemical characterization by XPS

In the first XPS analysis (Figure 2A) the intact TiO_2 coated surface was scanned and showed an almost stoichiometric TiO_2 composition: 46% oxygen, 18% titanium, 34% carbon and 1% nitrogen. Iron, cobalt and nickel were not detected, indicating complete coverage of the steel target by TiO_2.

The same target spot was analyzed after performing ten repeated SALDI measurements with 500 laser shots, each. The second surface analysis (Fig. 2B) showed no significant differences in the elementary composition: 43% oxygen, 12% titanium, 41% carbon, 3% nitrogen and 1% iron. After 5000 laser shots on the same target spot, the coating was damaged to a certain extent, but still enough TiO_2 was present to perform further SALDI measurements.

Carbon and the overstoichiometric amount of oxygen originate from hydrocarbon adsorbates from air, which deposit on the titanium oxide surface.

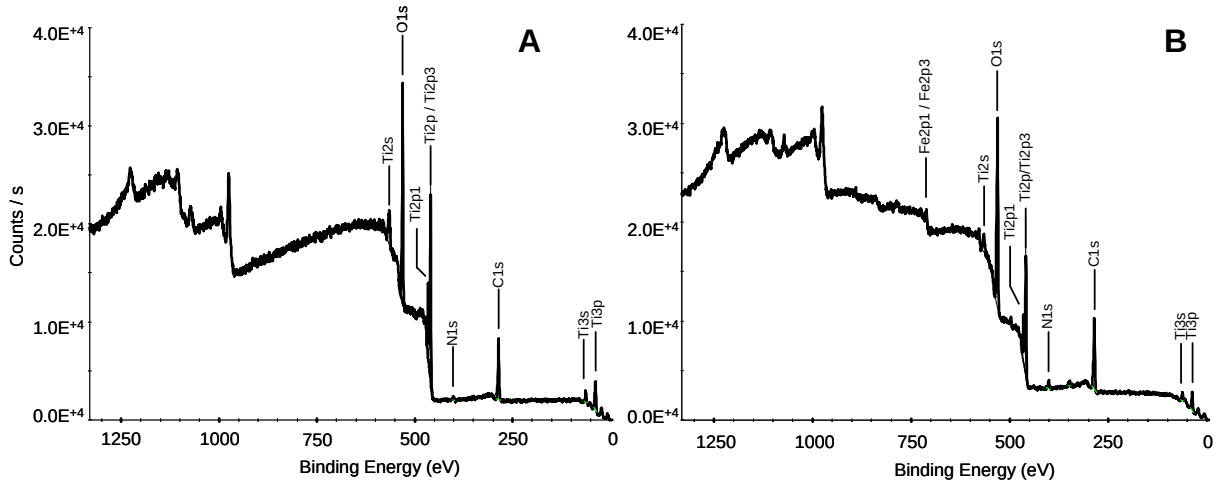

Fig. 2: XPS spectra of the TiO_2-coated target before (A) and after ten repeated LDI measurements (500 laser shots for each analysis). XPS spectra were acquired on a Thermo MultiLab 2000 spectrometer.

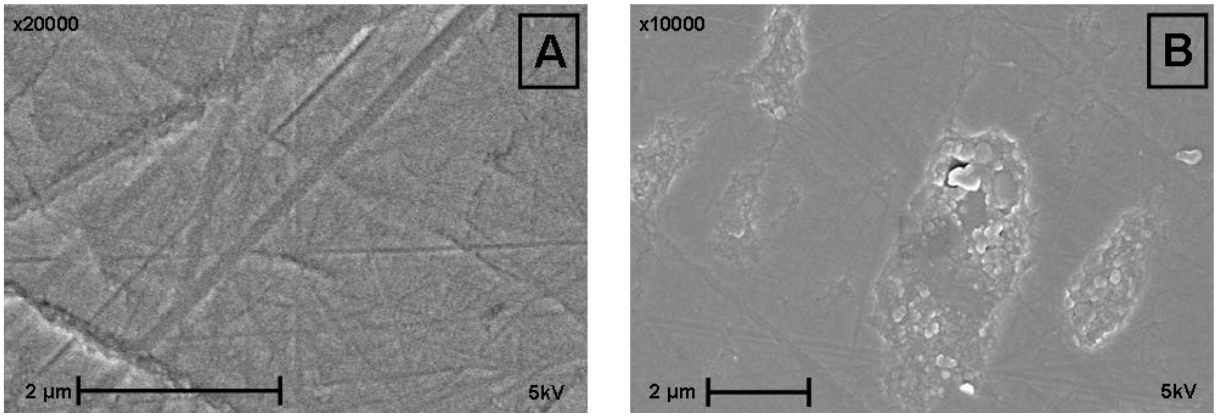

Fig. 3: SEM images of the intact 50 nm TiO_2 coating on a MALDI steel target (A) and after performing several LDI analysis with observable spallings (B).

3.1.2. Surface morphology investigation by SEM

To ascertain that the coating process was successful, the surface of the SALDI target was investigated by scanning electron microscopy (SEM). The SEM image (Figure 3A) shows that TiO_2 formed a layer completely covering the steel, but scratches were also visible. These scratches originated from the unevenness of the steel target surface, and because of the coating process, in which monolayer is superimposed to monolayer, so the scratches can still be detected even after coating a 50 nm TiO_2 layer.

No pores or formation of islands could be detected, proving the very evenly evaporation of TiO_2 on the steel surface.

After 10 repeated SALDI measurements, each 500 laser shots, slight ablations could be detected, but no complete depletion was noticed (Figure 3 B), and no significant diminishing of the ion signals occurred.

However, because the TiO_2 target could generate mass spectra of good quality with barely any background signals, it was proved that pores are not necessarily required for ion generation, the photocatalytic properties of TiO_2 solely initiate the ionization of the sample molecules.

3.1.3 SALDI analysis of the TiO_2 coated MALDI target

Whether organic or inorganic, each matrix used for MALDI MS analysis produces some background signals which usually are detected in the low-mass range (< 1000 *m/z*) hindering a satisfactory analysis of low-molecular-weight compounds. To determine the signals derived from the TiO_2 coated MALDI target, a SALDI analysis of the blank coated target was performed. In Figure 4, 500 laser shots at 50% laser intensity are summed. The two highest signals at *m/z* 23 and *m/z* 39 indicate the sodium and potassium ions. In the range from *m/z* 50 to 500, several weak signals occurred which could principally be assigned to titanium oxide compounds. No signal at *m/z* 48 was ob

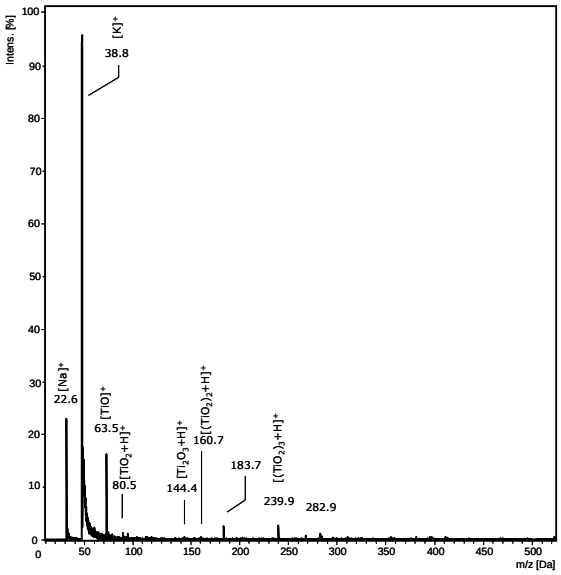

Fig. 4: LDI spectrum of blank TiO_2 target recorded on an Ultraflex I in positive mode

served, which would be caused by the titanium ion, whereas a quite strong signal at *m/z* 63.5 occurred, which could be $[TiO]^+$. In addition, $[TiO_2 + H]^+$, $[(TiO_2)_2 + H]^+$ and $[Ti_2O_3 + H]^+$ could be detected at *m/z* 80, *m/z* 144, *m/z* 161 and the trimer of TiO_2 at *m/z* 240. Furthermore, one signal at *m/z* 184 was observed which possibly represents $[(TiO_2)_2 + Na]^+$. One weak signal at *m/z* 283 could not be assigned.

One drawback of the TiO_2-coated target is that SALDI analysis can be performed only up to laser intensities of around 70 % of the maximum laser strength (max. 130 µJ). If the selected laser intensity is higher, the coating can spall resulting in non-interpretable spectra, caused by heterogeneous energy distribution leading to inhomogeneous desorption of analytes. The TiO_2-related interferences are, compared with the signals of the sample molecules, very weak and easy to assign. XPS and SEM analysis

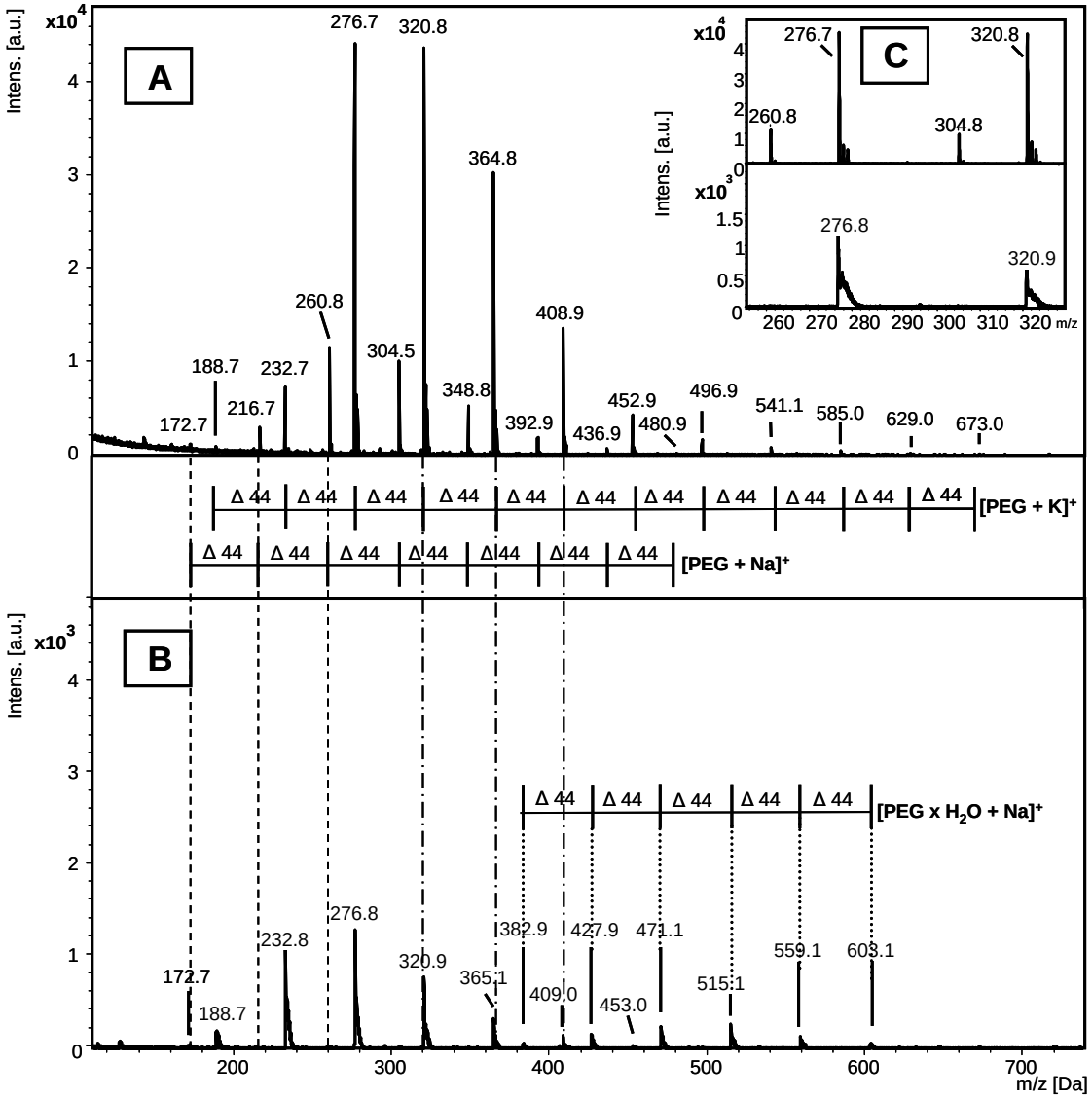

Fig. 5: LDI spectra of PEG 200, analyzed on the TiO_2 coated target (A), and TiO_2 nanoparticles as inorganic matrix (B), exhibiting abundant sodiated and potassiated ions but no protonated molecules. (C) shows an enlarged region of both spectra, demonstrating the more precise isotopic distribution in case of the TiO_2 coated target.

showed slight ablations of the TiO_2 layer after ten repeated SALDI measurements with 500 shots, each. This indicates that a thicker TiO_2 layer could be of advantage when the target is used for a large number of SALDI analyses, but limitations arise from the coating process in which a titanium filament is used. This filament undergoes high stress and decreases during deposition, and because of these extreme conditions, sooner or later the rod cracks, resulting in the abortion of the coating.

In general, the TiO_2 coating is not susceptible to solvents. But when sample solutions were prepared with TFA ratios higher than 1% ablation of the TiO_2 layer could be observed.

3.2. Comparative studies (PEG 200)

Kinumi et al. demonstrated the application of a TiO_2 particle suspension as inorganic matrix with low background noise in the lower mass region. [38]

Figure 5 shows the SALDI mass spectra of PEG 200 (average mass 200 Da) performed on the TiO_2-coated MALDI target (Figure 5A) compared to the same sample measured using a TiO_2 nanopowder suspension as energy absorbing substance (Figure 5B). For each spectrum 500 laser shots at exactly the same power (50% laser intensity) were summed.

The mass spectra of PEG 200 obtained by the use of the TiO_2-coated target (Figure 5A) had the following characteristics. The ions related to PEG 200 appeared as $[M + Na]^+$ at *m/z* 173, 217, 261, 305, 349, 393, 437, 481, 525 (n = 3-11) and $[M + K]^+$ at *m/z* 189, 233, 277, 321, 365, 409,

453, 497, 541, 585, 629, 673 (n = 3-14), which correspond to an adducts of the ubiquitous sodium or potassium ions. No protonated ions $[M + H]^+$ could be observed (here *n* represents the number of the oligomeric unit of PEG 200, $HO(CH_2CH_2O)_nH$). Potassiated ions were more than four times more abundant than the sodiated ions.

The mass spectra of PEG 200 obtained by use of TiO_2 as inorganic matrix (Fig. 5b) had the following characteristics: For the the sodiated ions $[M + Na]^+$ of PEG 200, only one signal could be detected: sodiated triethylene glycol at *m/z* 173, whereas seven potassiated ions $[M + K]^+$ at *m/z* 189, 233, 277, 321, 365, 409, 453 (n = 3-9) were identified. In this spectrum, several masses appeared different to the sodiated or potassiated ions of PEG 200, *m/z* 383, 428, 471, 515, 559, 603. These masses originate from the hygroscopic character of polyethyleneglycol, mapping these signals as $[M \times H_2O + Na]^+$. Because of the slower evaporation an accumulation of water on PEG 200 occurs, whereas when spotting directly on the TiO_2 layer, where no dispersant (glycerol) is needed to retain the analyte, this accumulation does not occur.

These spectra contained oligomeric distributions with a 44-u periodic pattern and no fragmentation within the repeating unit, only water addition could be detected in case of the inorganic TiO_2 powder.

When both spectra were compared, signal intensities for the TiO_2-coated target were up to 30-fold higher than the same measurement employing TiO_2 nanoparticles. Zooming the peak signals (Figure 5C) revealed a clear isotopic distribution for the TiO_2 layer. When TiO_2 nanoparticles were used, no isotopic distribution could be seen because of delayed extraction effects. These effects were caused by the inhomogeneous sample spot on the target and could be attributed to the use of inorganic matrices.

3.3. SALDI analysis of carbohydrates

Five different sugars were separately dissolved in water at an concentration of 1 µg/µL. The five solutions were combined at equal parts resulting in a final concentration of 200 ng/µL. One microlitre of the sample was spotted directly on the TiO_2-coated target and air dried. The mixture contained a pentose sugar (arabinose), a ketohexose (sorbose), a disaccharide (melibiose, D-Gal-α(1→6)-D-Glc), a trisaccharide (maltotriose) and a tetrasaccharide (maltotetraose), both linked with α-1,4 glycosidic bonds (Figure 6).

No protonated molecule peak could be observed, only strong cationization by sodium and potassium was obtained. Hence the molecular related ions of arabinose appeared as $[M + Na]^+$ at *m/z* 173 and as $[M + K]^+$ at *m/z* 189, the related ions of sorbose as $[M + Na]^+$ at *m/z* 203 and as $[M + K]^+$ at *m/z* 219. For melibiose, maltotriose and maltotetraose, again only the cationic signals of $[M + Na]^+$ at *m/z* 365, 527, 689 and $[M + K]^+$ at *m/z* 381, 543, 705 could be observed.

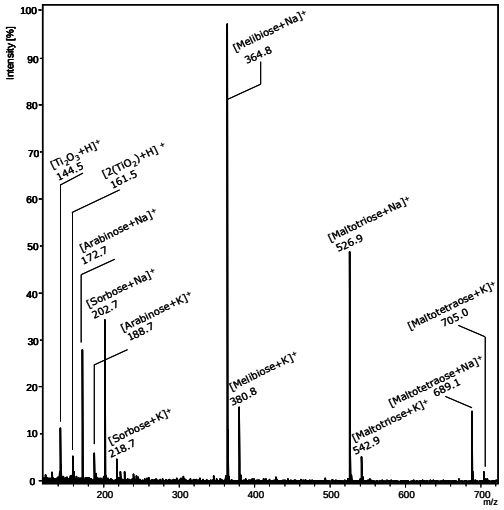

Fig. 6: SALDI spectrum of a mixture containing arabinose, sorbose, melibiose, maltotriose and maltotetraose employing a TiO_2 coated target.

3.4. Analysis of Amino acids

The suitability of the coated target was, furthermore, evaluated for the analysis of amino acids. First, the single amino acids were measured separately and after the successful detection was achieved (data not shown) the amino acids were combined, depending on their side chain classification.

For negatively charged amino acids, a SALDI analysis was performed in negative mode.

3.4.1. Non polar, aliphatic amino acids

For glycine and alanine, no protonated molecule signals (*m/z* 75, *m/z* 89) were detectable, but the $[M + Na]^+$ and $[M + K]^+$ ion peaks at *m/z* 98 and *m/z* 114 for glycine and *m/z* 112 and *m/z* 128 for alanine could be detected (Figure 7A). The other four non-polar, aliphatic amino acids were detected in their protonated, sodiated and potassiated forms. Proline turned out to be the most abundant amino acid in this class, even a quite strong signal from the protonated molecule was observed.

3.4.2. Aromatic amino acids

For each aromatic amino acid three signals could be clearly detected (Figure 7B), the protonated molecule signals at *m/z* 166, 188, 205, sodiated ions at *m/z* 188, 204, 226 and the potassiated ions at *m/z* 204, 219, 242. Ionization was strongest for the largest aromatic aminoacid, tryptophan. In comparison with the other groups of amino acids, because of the presence of alternating double bonds the peak intensity deriving from the aromatic amino acids was up to four times stronger.

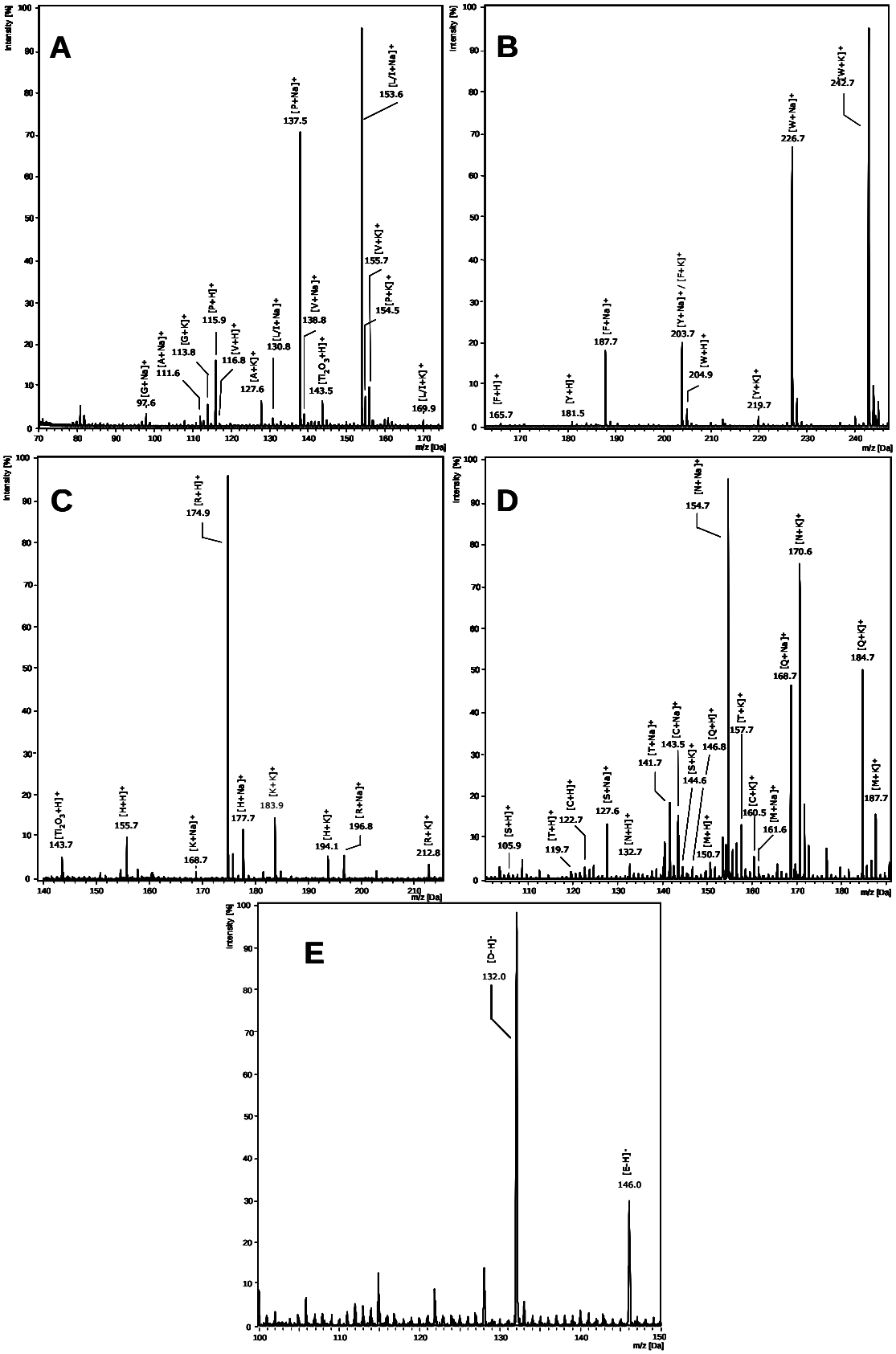

Fig. 7: SALDI analysis of non polar, aliphatic amino acids (A), aromatic amino acids (B), positively charged amino acids (C) and polar amino acids (D) in positive mode. Negatively charged amino acids were analyzed in negative mode (E). One letter code was used for all standard amino acids.

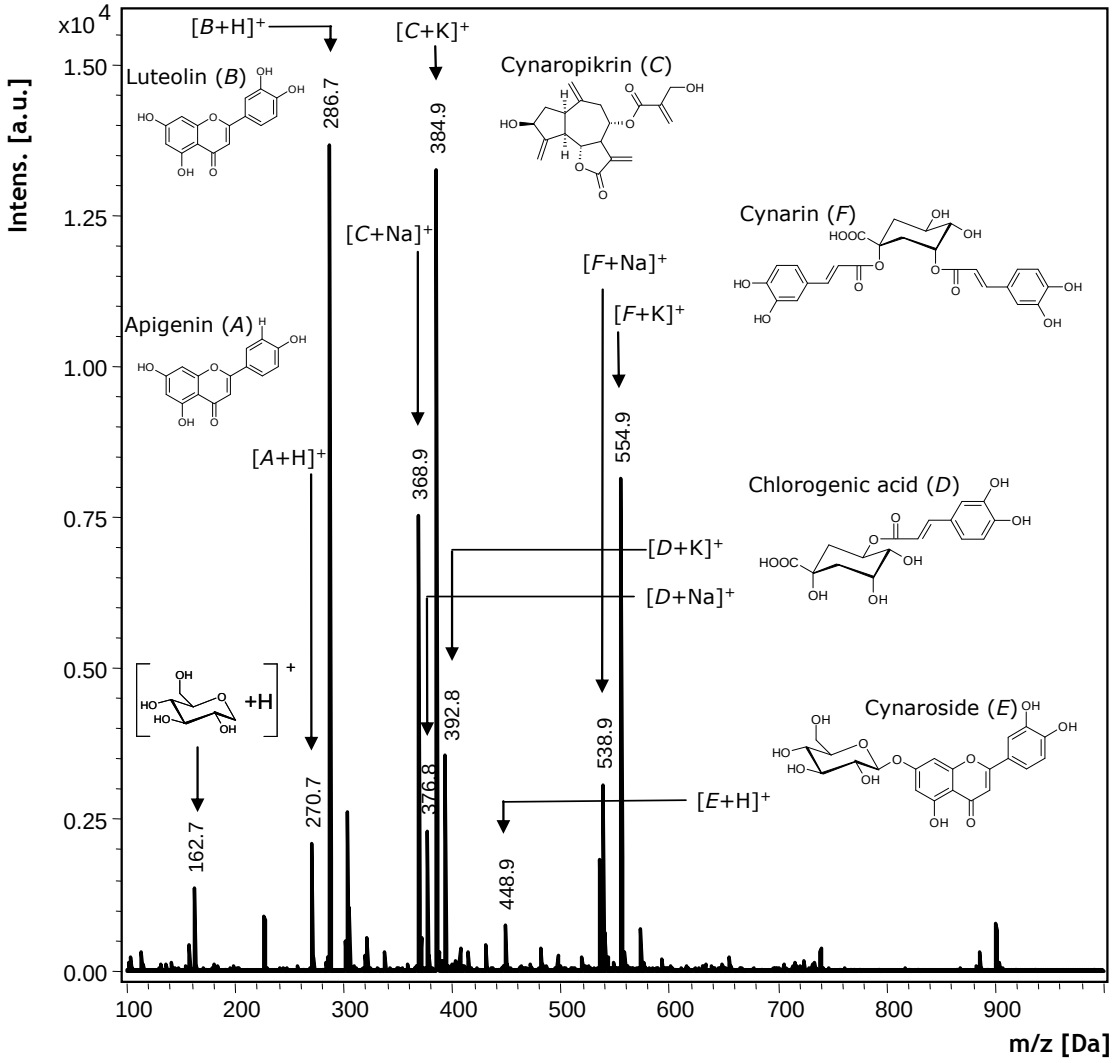

Fig. 8: LDI-MS spectrum of *Cynara scolymus* extract with detected Apigenin (A), Luteolin (B), Cynaropikrin (C), Chlorogenic acid (D), Cynaroside (E) and Cynarin (F), by averaging 500 laser shots.

3.4.3. Positively charged amino acids

In contrast to the other classes of amino acids, quite good ionization of the protonated molecular ions was detected for histidine and arginine (Figure 7C). For histidine, all three signals had more or less the same intensity. The signal intensity of the protonated arginine was, in contrast ten times higher than the signals of the sodiated or potassiated ions. No ionization of the protonated species was observed for lysine, whereas the sodiated and potassiated ions gave rather weak signals.

3.4.4. Polar amino acids

The mixture of all six polar amino acids resulted in a very complex spectrum because of the three signals for each amino acid (Figure 7D). Furthermore, for several ions the masses were different by just one Dalton making it difficult to determine the isotopic distribution of one ion and/or the signal of another. On balance, all three signals of every amino acid could be detected. For sodiated and potassiated asparagine and glutamine, ionization was five times higher than the other polar amino acids.

3.4.5. Negatively charged amino acids

No assignable signals could be recorded with SALDI analysis in the positive mode, whereas when switching to the negative mode and applying high laser intensities (Figure 7E), aspartic acid and glutamic acid could be detected in their negatively charged form, at *m/z* 132 and *m/z* 146. Although the intensities of the signals were quite low, they unequivocally originate from the two amino acids.

3.5. Determination of caffeoylquinic acids, flavonoids and cynaropikrin in Cynara scolymus extracts

The ingredients of *Cynara scolymus* are of nutritional value because exhibiting digestive properties, strengthening of the liver function, gall bladder function, and raising of HDL/LDL ratio. This reduces cholesterol levels, which diminishes the risk for arteriosclerosis and coronary heart disease. For the determination of active ingredients in *Cynara scolymus* it is important to have a rapid method for the qualitative identification of all substance classes present. Several HPLC methods have already been published [42-44], but one major disadvantage of these methods is that it usually takes more than 40 minutes for one measurement. The purpose of the SALDI analysis using the TiO_2-coated target was to develop a rapid method for the qualitative determination of caffeoylquinic acids, flavonoids and cynaropikrin in *Cynara scolymus* prior to qualitative analysis by HPLC. All four substance classes could be detected, the monocaffeoylquinic acids, dicaffeoylquinic acids, three flavonoids and one sesquiterpenlactone (Figure 8). The flavonoids apigenin, luteolin and cynaroside were ionized as $[M + H]^+$ at *m/z* 271, *m/z* 287 and *m/z* 449, cynaropikrin as $[M + Na]^+$ at *m/z* 369 and $[M + K]^+$ at *m/z* 385, chlorogenic acid as $[M + Na]^+$ at *m/z* 377 and $[M + K]^+$ at *m/z* 393 and cynarin as $[M + Na]^+$ at *m/z* 539 and $[M + K]^+$ at *m/z* 555. The signal at *m/z* 286 indicates luteolin but also the fragment of cynaroside lacking glucose. This glucose fragment was clearly indicated at *m/z* 163.

4. Conclusions

We have developed a new SALDI method for the analysis of small molecules using a conventional MALDI steel target coated with a 50 nm TiO_2 layer. This layer was built by electron beam evaporation. Because of this coating method, a very homogeneous layer with no pores or formation of islands could be achieved; evaporation of TiO_2 on the steel surface was very homogeneous. The layer was inspected with XPS to calculate the stoichiometric composition of the TiO_2 film. The stability of the layer was examined with SEM before and after repeated measurements on the same target area. Even after multiple measurements, no significant diminishing of the ion signals occurred. Slight ablation could be detected but still enough TiO_2 remained on the steel surface to perform further SALDI analysis. The layer also has no susceptibility to organic solvents, although it is susceptible to high laser intensity and high acid concentrations.

To determine the signals deriving from the TiO_2-coated MALDI target, blank SALDI analysis of the coated target was performed; this furnished a few signals only, which could mainly be assigned to titanium oxide compounds. However the signals deriving from the titanium compounds were of low intensities compared with the signals from the sample spots, and did not, therefore, hinder the SALDI analysis. Also, comparison of the TiO_2-coated target and TiO_2 nanopowder as inorganic matrix was performed using PEG 200 as sample. The TiO_2 coated target resulted in up to 30-fold higher signal intensity compared with the inorganic matrix. Furthermore, no delayed extraction effects occurred during the measurements, resulting in a clear isotopic distribution. Because sample spotting does not require any dispersant, evaporation was very fast, so no addition of water occurred, resulting in a simplified spectral interpretation.

Five different sugars were successfully analyzed, and the resulting SALDI spectrum showed strong cationization by sodium and potassium; no protonated peaks could be observed. For each sugar, the ratio of the intensities of the sodiated and potassiated ions was approximately 6:1. After the positive detection of every single amino acid, these were combined depending on their side-chain classification and once more a SALDI measurement was performed. To some extent, the resulting spectra were very complex, but again every amino acid could be identified. In a final analysis, an extract from *Cynara Scolymus* was spotted on the TiO_2-coated target, with the objective of non-time consuming, qualitative analysis of the ingredients. All three of the flavonoids detected were ionized as their protonated ions, whereas all other compounds were ionized as $[M + Na]^+$ and $[M + K]^+$.

We have proved that the TiO_2-coated target has a large generality in ionizing, in addition the quick and simple sample preparation could, in some applications, make this technique an ideal choice for the qualitative analysis of metabolites. Furthermore, the TiO_2 coating provides a taarget reusable many times for SALDI measurements.

Acknowledgements

This work was supported by the Austrian Proteomics Platform APP (Vienna, Austria) and by the SpezialForschungsBereich SFB (Vienna, Austria). The authors thank Dr. Kristian Pfaller from the department of Embriology and Histology of the Medical University of Innsbruck for the preparation of the SEM data, and the Bionorica Company for the provision of the *Cynara Scolymus* extracts.

References

[1] Hillenkamp F, Karas M, Beavis RC, Chait BT (1991) Matrix-assisted laser desorption/ionization mass spectrometry of biopolymers. Anal Chem 63 (24):1193A-1203A

[2] Karas M, Bachmann D (1987) Matrix-assisted ultraviolet laser desorption of non-volatile compounds. International Journal of Mass Spectrometry and Ion Processes 78:53-68

[3] Karas M, Hillenkamp F (1988) Laser desorption ionization of proteins with molecular masses exceeding 10,000 daltons. Anal Chem 60 (20):2299-2301

[4] Busch KL (1999) Matrices for MALDI. Spectroscopy 14 (9):14-16

[5] Beavis RC, Chaudhary T, Chait BT (1992) α-Cyano-4-hydroxycinnamic acid as a matrix for matrixassisted laser desorption mass spectromtry. Organic Mass Spectrometry 27 (2):156-158

[6] Strupat K, Karas M, Hillenkamp F (1991) 2,5-Dihydroxybenzoic acid: a new matrix for laser desorption—ionization mass spectrometry International Journal of Mass Spectrometry and Ion Processes 111:89-102

[7] Tanaka HWK (1988) Protein and polymer analyses up to m/z 100 000 by laser ionization time-of-flight mass spectrometry. T Rapid Commun Mass Spectrom (2):151-153

[8] Yalcin T, Wallace WE, Guttman CM, Li L (2002) Metal powder substrate-assisted laser desorption/ionization mass spectrometry for polyethylene analysis. Anal Chem 74 (18):4750-4756

[9] Schürenberg M, Hillenkamp F, Dreisewerd K (1999) Laser Desorption/Ionization Mass Spectrometry of Peptides and Proteins with Particle Suspension Matrixes. Anal Chem 71 (1):221-229

[10] Dale MJ, Knochenmuss R (1997) Graphite/liquid mixed matrices for laser desorption/ionization mass spectrometry. Anal Chem 68:3321

[11] Dale MJ, Knochenmuss R (1997) Two-phase Matrix-assisted Laser Desorption/Ionization: Matrix Selection and Sample Pretreatment for Complex Anionic Analytes. Rapid Commun Mass Spectrom 11 (1):136-142

[12] Sunner J, Dratz E, Chen YC (1995) Graphite surface-assisted laser desorption/ionization time-of-flight mass spectrometry of peptides and proteins from liquid solution. Anal Chem 67 (23):4335-4342

[13] Alimpiev S, Nikiforov S (2001) On the mechanism of laser-induced desorption–ionization of organic compounds from etched silicon and carbon surfaces. Journal of Chemical Physics 115 (4):1891-1901

[14] Zenobi R, Knochenmuss, R. (1998) Ion formation in MALDI mass spectrometry. Mass Spectrometry Reviews 17 (5):337-366

[15] Crecelius A, Clench MR, Richards DS, Parr V (2002) Thin-layer chromatography-matrix-assisted laser desorption ionisation-time-of-flight mass spectrometry using particle suspension matrices. J Chromatogr A 958 (1-2):249-260

[16] Kawasaki H, Sugitani, T., Watanabe, T., Yonezawa T., Moriwaki H., Arakawa R. (2008) Layer-by-Layer Self-Assembled Mutilayer Films of Gold Nanoparticles for Surface-Assisted Laser Desorption/Ionization Mass Spectrometry. Anal Chem 80 (19):7524-7533

[17] Michalak L (1994) C60-assisted laser desorption/ionization mass spectrometry in the analysis of phosphotungstic acid. Org Mass Spectrom 29:512

[18] Huang JP, Yuan CH, Shiea J, Chen YC (1999) Rapid screening for diuretic doping agents in urine by C60-assisted laser-desorption-ionization-time-of-flight mass spectrometry. J Anal Toxicol 23 (5):337-342

[19] Szabo Z, Vallant RM, Takatsy A, Bakry R, Najam-ul-Haq M, Rainer M, Huck CW, Bonn GK Laser desorption/ionization mass spectrometric analysis of small molecules using fullerene-derivatized silica as energy-absorbing material. J Mass Spectrom 45 (5):545-552

[20] Armstrong DW, Zhang LK, He L, Gross ML (2001) Ionic liquids as matrixes for matrix-assisted laser desorption/ionization mass spectrometry. Anal Chem 73 (15):3679-3686

[21] Li YL, Gross ML (2005) Ionic-Liquid Matrices for Improved Analysis of Phospholipids by MALDI-TOF Mass Spectrometry Journal of the American Society for Mass Spectrometry 16 (5):679-682

[22] Najam-ul-Haq M, Rainer M, Huck CW, Hausberger P, Kraushaar H, Bonn GK (2008) Nanostructured diamond-like carbon on digital versatile disc as a matrix-free target for laser desorption/ionization mass spectrometry. Anal Chem 80 (19):7467-7472

[23] Shen Z, Thomas JJ, Averbuj C, Broo KM, Engelhard M, Crowell JE, Finn MG, Siuzdak G (2001) Porous silicon as a versatile platform for laser desorption/ionization mass spectrometry. Anal Chem 73 (3):612-619

[24] Wei J, Buriak JM, Siuzdak G (1999) Desorption/Ionization Mass Spectrometry on Porous Silicon. Nature 399:243-246

[25] Zhang Q, Zou H, Guo Z (2001) Matrix-assisted laser desorption/ionization mass spectrometry using porous silicon and silica gel as matrix. Rapid Commun Mass Spectrom 15 (3):217-223

[26] Cuiffi JD, Hayes DJ, Fonash SJ, Brown KN, Jones AD (2001) Desorption-ionization mass spectrometry using deposited nanostructured silicon films. Anal Chem 73 (6):1292-1295

[27] Okuno S, Wada Y, Arakawa R (2005) Quantitative analysis of polypropyleneglycol mixtures by desorption/ionization on porous silicon mass spectrometry International Journal of Mass Spectrometry 241 (1):43-48

[28] Alimpiev S, Grechnikov A, Sunner J, Karavanskii V, Simanovsky Y, Zhabin S, Nikiforov S (2008) On the role of defects and surface chemistry for surface-assisted laser desorption ionization from silicon. J Chem Phys 128 (1):014711

[29] Kruse RA, Rubakhin SS, Romanova EV, Bohn PW, Sweedler JV (2001) Direct assay of Aplysia tissues and cells with laser desorption/ionization mass spectrometry on porous silicon. J Mass Spectrom 36 (12):1317-1322

[30] Kruse RA, Li X, Bohn PW, Sweedler JV (2001) Experimental factors controlling analyte ion generation in laser desorption/ionization mass spectrometry on porous silicon. Anal Chem 73 (15):3639-3645

[31] Okuno S, Oka K, Arakawa R (2005) Oxidation of ferrocene derivatives in desorption/lonization on porous silicon. Anal Sci 21 (12):1449-1451

[32] Okuno S, Arakawa R, Okamoto K, Matsui Y, Seki S, Kozawa T, Tagawa S, Wada Y (2005) Requirements for laser-induced desorption/ionization on submicrometer structures. Anal Chem 77 (16):5364-5369

[33] Arakawa R, Shimomae Y, Morikawa H, Ohara K, Okuno S (2004) Mass spectrometric analysis of low molecular mass polyesters by laser desorption/ionization on porous silicon. J Mass Spectrom 39 (8):961-965

[34] Trauger SA, Go EP, Shen Z, Apon JV, Compton BJ, Bouvier ES, Finn MG, Siuzdak G (2004) High sensitivity and analyte capture with desorption/ionization mass spectrometry on silylated porous silicon. Anal Chem 76 (15):4484-4489

[35] Lewis WG (2003) Desorption/ionization on silicon (DIOS) mass spectrometry: background and applications. International Journal of Mass Spectrometry 226 (1):107-116

[36] Go EP, Apon JV, Luo G, Saghatelian A, Daniels RH, Sahi V, Dubrow R, Cravatt BF, Vertes A, Siuzdak G (2005) Desorption/ionization on silicon nanowires. Anal Chem 77 (6):1641-1646

[37] Ren SF, Zhang L, Cheng ZH, Guo YL (2005) Immobilized carbon nanotubes as matrix for MALDI-TOF-MS analysis: applications to neutral small carbohydrates. J Am Soc Mass Spectrom 16 (3):333-339

[38] Kinumi T, Saisu T, Takayama M, Niwa H (2000) Matrix-assisted laser desorption/ionization time-of-flight mass spectrometry using an inorganic particle matrix for small molecule analysis. J Mass Spectrom 35 (3):417-422

[39] Chen CT, Chen YC (2004) Desorption/ionization mass spectrometry on nanocrystalline titania sol-gel-deposited films. Rapid Commun Mass Spectrom 18 (17):1956-1964

[40] Bi H, Qiao L, Busnel JM, Devaud V, Liu B, Girault HH (2009) TiO(2) printed aluminum foil: single-use film for a laser desorption/ionization target plate. Anal Chem 81 (3):1177-1183

[41] Yuan M, Shan Z, Tian B (2005) Preparation of highly ordered mesoporous WO3–TiO2 as matrix in matrix-assisted laser desorption/ionization mass spectrometry Microporous and Mesoporous Materials 78 (1):37-41

[42] Schütz K, Persike M (2006) Characterization and quantification of anthocyanins in selected artichoke (Cynara scolymus L.) cultivars by HPLC–DAD–ESI–MSn. Anal Bioanal Chem 384 (7-8):1511-1517

[43] Schütz K, Kammerer D, Carle R, Schieber A (2004) Identification and quantification of caffeoylquinic acids and flavonoids from artichoke (Cynara scolymus L.) heads, juice, and pomace by HPLC-DAD-ESI/MS(n). J Agric Food Chem 52 (13):4090-4096

[44] Wang M, Simon JE, Aviles IF, He K, Zheng QY, Tadmor Y (2003) Analysis of antioxidative phenolic compounds in artichoke (Cynara scolymus L.). J Agric Food Chem 51 (3):601-608